Size Effects in Thermal Conduction by Phonons

Philip B. Allen[1,*]

[1] *Physics and Astronomy Department, Stony Brook University, Stony Brook, NY 11794-3800, USA*

(Dated: May 20, 2014)

Heat transport in nanoscale systems is both hard to measure microscopically, and hard to interpret. Ballistic and diffusive heat flow coexist, adding confusion. This paper looks at a very simple case, not achievable experimentally. This is a nanoscale crystal repeated periodically. Not just the structure is constrained by periodic boundary conditions, but also the heat flow. The distinction between ballistic and diffusive transport disappears. A non-local Fourier relation between current $J(x)$ and temperature $\nabla T(x')$ is established. Nanoscale effects are described by a straightforward extension of standard quasiparticle gas theory of bulk solids. As a further simplification, one-dimensional flow is studied in a (three-dimensional) supercell of length L, conceptually divided into N parallel planar segments enumerated by ℓ. External heat enters chosen segments uniformly at rates $\dot{e}(\ell)$, and leaves other segments uniformly. Such systems are popular models for simulation of bulk heat transport using classical molecular dynamics (MD). Heat flow is affected by the fact that the phonon carriers of heat have mean free paths comparable to the spatial scale of the heating and cooling. When such systems are used to model bulk conductivity, nanoscale aspects alter answers. These aspects arise from finite computer resources that limit system size. These nanoscale effects are undesirable, and need to be avoided by extrapolation. The reverse point of view is that nanoscale effects are seen here in their simplest form. An analysis is given, based on the Peierls-Boltzmann equation. Calculations using generalized Debye models show that extrapolation requires fractional powers of $1/L$. It is also argued that heating and cooling should be distributed sinusoidally ($\dot{e} \propto \cos(2\pi x/L)$) to improve convergence of numerics. It is possible that this analysis has implications about finite size effects that could be extended to actual nanoscale systems of less mathematical simplicity.

PACS numbers: 66.70.-f, 63.22.-m, 65.80.-g

I. INTRODUCTION

The linear (Fourier) relation between heat current J_x and temperature gradient $\nabla_x T$ must be non-local[1] unless the distance scale of temperature variation exceeds the carrier mean-free path Λ. The time-independent steady state version,

$$J_x(x) = -\int dx' \kappa(x,x') \nabla_{x'} T(x') \qquad (1)$$

reduces to the usual Fourier law $J_x = -\kappa_0 \nabla_x T$ if the system is spatially homogeneous, and the temperature gradient has negligible spatial variation on the scale of Λ. This is the usual situation in a macroscopic measurement on a homogeneous sample. In this limit, $\kappa(x,x') = \kappa(x-x')$, and $\kappa_0 = \int dx \kappa(x)$. In the homogeneous case, assuming a long sample, Fourier variables are appropriate. The linear relation is then $J_x(k) = -\kappa(k)\nabla_x T(k)$. For a homogeneous temperature gradient, the experiment is described by the $k = 0$ Fourier component, and $\kappa_0 = \lim_{k\to 0} \kappa(k)$.

Nanoscale systems have boundaries that add complexity[2–5]. There is an argument[6] that says the Fourier law does not apply in all cases. This paper avoids such issues, and addresses a case where the complexity is minimized, namely, a homogeneous nanoscale system with periodic boundary conditions. This is not achievable experimentally, but is a preferred geometry for simulation of heat transport by classical molecular dynamics (MD) using the "direct method"[7–11]. Heat is introduced locally, extracted locally some distance away, and temperature is monitored in between. The aim of the modeling is usually to extract the conductivity of a macroscopic sample. Nanoscales automatically enter, because the computer cannot process atomic information on a macroscopic scale. An interesting simplification is that, having no boundary, the distinction between ballistic and diffusive transport has no relevance to the calculation.

A very nice example was given by Zhou *et al.*[10], who carefully analyze computational accuracy, using the semiconductor GaN as an example. The large thermal conductivity (several hundred W/mK at room temperature) indicates that the dominant acoustic phonons have mean free paths Λ_Q of order hundreds of interatomic spacings a. Since acoustic phonon mean free paths increase rapidly as wave-vector $\vec{Q} \to 0$, a significant amount of heat is carried by phonons with much longer mean free paths, thousands in units of a. The simulations were done for periodic cells up to length $L \approx 1000a$. Probably another factor of 10 in length would be required to fully converge the answers. At a series of lengths $L < 1000A$, conductivity $\kappa_{\rm eff}(L)$ was extracted as the ratio $-J_x/\nabla_x T$, where the temperature gradient was determined at $x = \pm L/4$, half way between the heat source and sink. Extrapolation of $\kappa_{\rm eff}(L)$ to $L \to \infty$ (assuming $\kappa_{\rm eff}(L) - \kappa_{\rm bulk} \propto 1/L$) indicated that the value of $\kappa_{\rm bulk}$ was typically twice bigger than the maximum achieved value $\kappa_{\rm eff}(L \approx 1000a)$. Zhou *et al.*[10] discover evidence of

a breakdown in this method of extrapolation.

Refs. 8,10,and 11 all use periodic boundary conditions. The simplicity of the periodic boundary means that phonon gas theory can be easily adapted to this nanoscale situation. Here I offer such an analysis. The result suggests that $\kappa_{\rm eff}(L)-\kappa_{\rm bulk}\propto 1/\sqrt{L}$ should give a better extrapolation. The analysis also points to a better algorithm for adding and removing heat.

II. SEGMENTED PERIODIC SLAB MODEL

Fig. 1 is a cartoon system ("simulation cell" of N "slabs") as might be employed in a classical MD calculation. The primary variables are the imposed rate of heating $\dot{e}(\ell)$ of the ℓ'th slab, and the "measured" slab temperature $T(\ell)$ (mean kinetic energy of the atoms in the slab, divided by $3k_B/2$). These primary variables coincide with the quantities measured in heat conduction experiments. The secondary variables are the heat flux $J_x(\ell+\frac{1}{2})$ and the temperature gradient $\nabla_x T(\ell+\frac{1}{2})$; both are defined at the junction of slabs ℓ and $\ell+1$. The secondary variables are related to the primary variables by the two fundamental slab-ring equations,

$$\nabla_x T(\ell+\frac{1}{2}) = [T(\ell+1)-T(\ell)]/A \tag{2}$$

$$\dot{e}(\ell) = [J_x(\ell+\frac{1}{2}) - J_x(\ell-\frac{1}{2})]/A \tag{3}$$

where A is the width of the slab. Eq.(3) is just energy conservation. In order to allow a steady state, it is required that $\sum_\ell \dot{e}(\ell)=0$, meaning that no net heating occurs.

The relation between heat flux and temperature gradient, in linear approximation, is

$$J_x(\ell+\frac{1}{2}) = -\sum_{m=0}^{N-1}\kappa(\ell-m)\nabla_x T(m+\frac{1}{2}) \tag{4}$$

This is the analog of Eq.(1). The position variable x has been discretized into the slab index ℓ. The thermal conductivity is similarly discretized. In terms of these discrete and periodic variables, the form of Eq.(4) is required by the linear approximation. The matrix $\kappa(\ell,m)$ is rigorously defined. It is independent of the heating $\dot{e}(\ell)$. If the slabs are identical, then $\kappa(\ell,m)$ retains the N-fold translational symmetry of the ring. Therefore $\kappa(\ell+n,m+n)=\kappa(\ell,m)=\kappa(\ell-m,0)\equiv\kappa(\ell-m)$. All variables are N-fold periodic in ℓ, including the nonlocal conductivity $\kappa(\ell)=\kappa(\ell+N)$.

Conjugate to the N positions on the ring are N Fourier vectors $q=(2\pi/N)n_q$. I will always use k for the Fourier transform of the continuous variable x, and q for the discrete case. This notation then clarifies that $\kappa(k)$ refers to thermal conductivity of a large homogeneous system, and $\kappa(q)$ to the small but periodically repeated supercell.

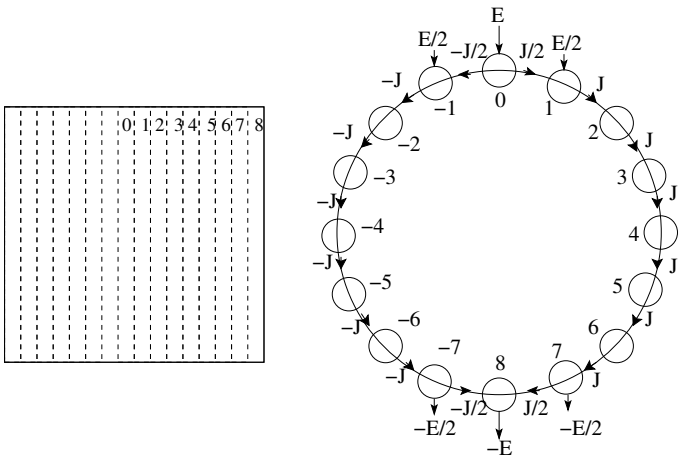

FIG. 1. Two schematics of a periodic supercell used for MD modeling of thermal conductivity. The cell is divided into N slabs (here $N=16$) in the direction x of heat flow. It is periodically repeated in all three directions. Heat is randomly inserted as impulses on randomly chosen atoms in slab 0. Equal random extraction of heat occurs in slab $N/2$. Thus the heat current density is controlled. Temperature is measured in slabs $1,2,\ldots,N/2-1$, and also in the similar slabs $-1,-2,\ldots$. The temperature gradient is minimum in slab $N/4$ and $3N/4$. From these gradients, the value of $\kappa_{\rm eff}(N)$ is evaluated.

Just as the integers ℓ are defined *modulo* N, similarly the integers n_q have the same periodicity, $n_q+N=n_q$. The Fourier representation of the discretized variables is particularly simple and convenient:

$$\begin{aligned}
\dot{e}(\ell) &= \sum_q e^{iq\ell}\dot{e}(q)\\
T(\ell) &= \sum_q e^{iq\ell}T(q)\\
J_x(\ell+\frac{1}{2}) &= \sum_q e^{iq(\ell+\frac{1}{2})}J_x(q)\\
\nabla_x T(\ell+\frac{1}{2}) &= \sum_q e^{iq(\ell+\frac{1}{2})}\nabla_x T(q)\\
\kappa(\ell) &= \sum_q e^{iq\ell}\kappa(q),
\end{aligned} \tag{5}$$

where sums go over the N distinct values of q. The reverse transforms are

$$\begin{aligned}
\dot{e}(q) &= \frac{1}{N}\sum_\ell e^{-iq\ell}\dot{e}(\ell)\\
J_x(q) &= \frac{1}{N}\sum_\ell e^{-iq(\ell+\frac{1}{2})}J_x(\ell+\frac{1}{2}),
\end{aligned} \tag{6}$$

and similar for T, $\nabla_x T$, and κ. Sums go over the N distinct values of ℓ. The Fourier version of Eq.(4) is

$$J_x(q) = -\kappa(q)\nabla_x T(q) \tag{7}$$

III. PHONON GAS THEORY

This section assumes a macroscopic homogeneous ("continuum") solid. The next section translates this to a segmented supercell of periodic ("discrete") slabs. The short-hand Q, in both continuum and discrete models, denotes $(\vec{Q}, s)$, the (three-dimensional) wavevector $\vec{Q}$ and the branch index s of the phonons. Spatial variation is driven by external heating and is assumed to occur only in the x direction. Thermal properties are described by $N_Q(x)$, the mean occupation of mode Q at (one-dimensional) position x. The heat current is

$$J_x(x) = \frac{1}{\Omega}\sum_Q \hbar\omega_Q v_{Qx} N_Q(x), \tag{8}$$

The Peierls-Boltzmann equation (PBE)[12,13] describes the dynamics of $N_Q(x)$. Anharmonic phonon events drive N_Q to the local thermal equilibrium Bose-Einstein distribution $n_Q = 1/(\exp(\hbar\omega_Q/k_BT(x)) - 1)$. Spatial variations in $N_Q(x,t)$ change by phonon drift with velocity $\vec{v}_Q = \partial\omega_Q/\partial\vec{Q}$. In steady state, N_Q is stationary,

$$\frac{\partial N_Q}{\partial t} = 0 = \left(\frac{\partial N_Q}{\partial t}\right)_{\rm drift} + \left(\frac{\partial N_Q}{\partial t}\right)_{\rm collisions}. \tag{9}$$

Writing N_Q as the sum of a local equilibrium $n_Q(T(x))$ (unaffected by collisions) and a deviation $\Phi_Q(x)$, the drift term of the PBE has two contributions, $-(\partial n_Q/\partial T)v_{Qx}\nabla_x T$ and $-v_{Qx}\nabla_x\Phi_Q$. The second of these is negligible when the temperature gradient is constant, but becomes important when there is spatial inhomogeneity. The collision term, after linearization, has the form $-\sum_{Q'} C_{QQ'}\Phi_{Q'}$, where $C_{QQ'}$ is a complicated collision operator. To first approximation (the "relaxation time approximation," RTA) this can be written as $-\Phi_Q/\tau_Q$, where $1/\tau_Q$ is the "single mode relaxation rate," meaning the thermalization rate (or life-time broadening) of mode Q that appears if only that one mode is out of equilibrium. The PBE then takes the form

$$[v_{Qx}\nabla_x + 1/\tau_Q]\Phi_Q(x) = -v_{Qx}\frac{\partial n_Q}{\partial T}\nabla_x T \tag{10}$$

In the continuum picture, the Fourier relations are $\Phi_Q(x) = (1/2\pi)\int dk \exp(ikx)\Phi_Q(k)$ and $\Phi_Q(k) = \int dx \exp(-ikx)\Phi_Q(x)$. The PBE becomes

$$(ikv_{Qx} + 1/\tau_Q)\Phi_Q(k) = -v_{Qx}\frac{\partial n_Q}{\partial T}\nabla_x T(k). \tag{11}$$

The thermal conductivity $\kappa(k)$ in continuous k space obeys the Fourier transformed version of Eq.(1), $J_x(k) = -\kappa(k)\nabla_x T(k)$, and has the form

$$\kappa(k) = \frac{1}{\Omega}\sum_Q \frac{\hbar\omega_Q v_{Qx}^2(\partial n_Q/\partial T)}{1/\tau_Q + ikv_{Qx}} \tag{12}$$

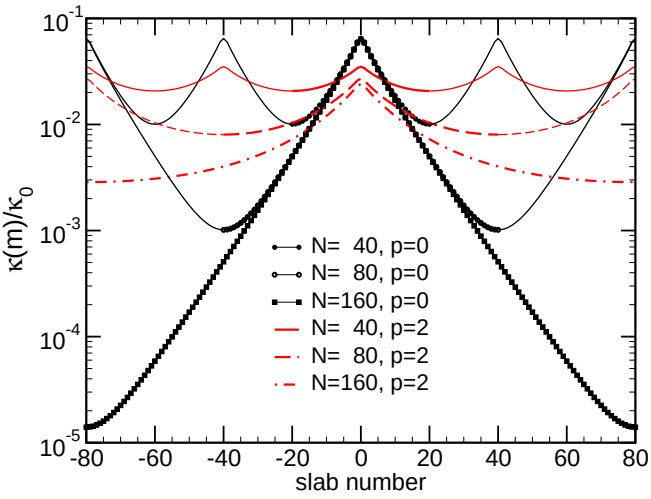

FIG. 2. The non-local thermal conductivity, $\kappa(m)$ defined in Eq.(4), and computed using Eq.(31) for the slab model, Fourier transformed back to coordinate space. The minimum mean free path $\Lambda_{\rm min}$ is $10A$; the supercell has N slabs of width A, where N is shown in the figure legend. The period N repetitions are shown. Black and red curves use the power law $p = 0, 2$ respectively of $\Lambda_Q = \Lambda_{\rm min}(\omega_D/\omega_Q)^p$.

This can be Fourier-transformed back to x-space:

$$\kappa(x - x') = \frac{1}{\Omega}\sum_Q^{v_{Qx}>0} \hbar\omega_Q v_{Qx} e^{-|x-x'|/v_{Qx}\tau_Q}. \tag{13}$$

This uses the property that $\vec{v}_Q$ changes sign when $\vec{Q}$ changes sign.

The result Eq.(13) shows explicitly that heat transport is influenced non-locally by temperature variations. The velocity $|v_{Qx}|$ is bounded, but the free path $|v_{Qx}|\tau_Q$ is not. Relaxation times of long wavelength acoustic phonons diverge as $|\vec{Q}| \to 0$. In the over-simplified model where every phonon Q has the same relaxation rate $1/\tau_Q = 1/\tau_0$, the Q-integrated $\kappa(x)$ decays exponentially as $\exp(-|x|/\Lambda_0)$. However, in reality the divergence of τ_Q causes a slower decay. The exponential decay (when $1/\tau_Q$ is replaced by $1/\tau_0$) is illustrated in Fig. 2, but for the segmented periodic case, described in the next section. Also shown is the non-exponential decay found when $1/\tau_Q \propto \omega_Q^{-2}$.

IV. GAS THEORY ON THE SEGMENTED PERIODIC SLAB

Gas theory translates to the segmented supercell in a slightly awkward way. Temperature $T(\ell)$ is a slab property, but current $J_x(\ell+\frac{1}{2})$ is a junction property. Gas theory has temperature as a primary variable, so $T(\ell)$ should correspond to $T(x)$ averaged over the ℓ'th slab. Evidently $N_Q(\ell)$ is a slab property, not a junction property. But

since the current in gas theory is $\sum_Q \hbar\omega_Q v_{Qx} N_Q/\Omega$, we are forced to compromise and define

$$J_x(\ell+\frac{1}{2}) = \frac{1}{\Omega}\sum_Q \hbar\omega_Q v_{Qx}\frac{N_Q(\ell)+N_Q(\ell+1)}{2}. \quad (14)$$

Transforming to the discrete slab Fourier representation, this becomes

$$J_x(q) = \frac{1}{\Omega}\sum_Q \hbar\omega_Q v_{Qx}\cos(q/2)\Phi_Q(q). \quad (15)$$

Similarly, the temperature gradient, Eq.(2), in Fourier variables, is

$$\nabla_x T(q) = 2i\sin(q/2)T(q), \quad (16)$$

and the fundamental connection Eq.(3) between heat input and current is

$$\dot{e}(q) = 2i\sin(q/2)J(q). \quad (17)$$

In these equations, the slab thickness A has been set to 1 (*i.e.* it is the unit of length.) The discrete slab index ℓ corresponds to a length ℓA. The discrete slab Fourier vector q corresponds to a physical wavevector $(2\pi/NA)n_q$, where $NA = L$ is the length of the supercell.

The remaining task is to translate Eq.(12) to slab language. The ingredient needing translation is ∇_x which appears twice in Eq.(10). The translation of this equation is

$$\begin{aligned}\Phi_Q(\ell) &= \theta(v_{Qx})v_{Qx}\tau_Q \\ &\times\left[\frac{\partial n_Q}{\partial T}(T(\ell-1)-T(\ell))+(\Phi_Q(\ell-1)-\Phi_Q(\ell)\right] \\ &+\theta(-v_{Qx})v_{Qx}\tau_Q \\ &\times\left[\frac{\partial n_Q}{\partial T}(T(\ell)-T(\ell+1))+(\Phi_Q(\ell)-\Phi_Q(\ell+1)\right].\end{aligned} \quad (18)$$

The meaning is that drift entering slab ℓ from the left uses positive velocity phonons which carry information from the slab on the left, while drift entering slab ℓ from the right uses negative velocity phonons bringing information from the slab on the right.

The discretized PBE, Eq.(18) can be solved in discrete Fourier space, giving

$$\begin{aligned}\Phi_Q(q) &= \frac{v_{Qx}\tau_Q(\partial n_Q/\partial T)S(q)}{1+2i\sin(q/2)v_{Qx}\tau_Q S(q)} \\ &= \Re\left[\frac{v_{Qx}\tau_Q(\partial n_Q/\partial T)}{e^{iq/2}+2i\sin(q/2)v_{Qx}\tau_Q}\right]\end{aligned} \quad (19)$$

In the first line of Eq.(19), the factor $S(q)$ is $\exp(-iq/2)$ if v_{Qx} is positive and $\exp(iq/2)$ if v_{Qx} is negative. The second line follows from symmetries under $\vec{Q}\to-\vec{Q}$. Finally, this gives the answer for the discrete slab gas theory thermal conductivity,

$$\begin{aligned}\kappa(q) &= \frac{1}{\Omega}\sum_Q \hbar\omega_Q\frac{\partial n_Q}{\partial T}v_{Qx}^2\tau_Q\cos(q/2) \\ &\times\Re\left[\frac{1}{e^{iq/2}+2i\sin(q/2)v_{Qx}\tau_Q}\right]\end{aligned} \quad (20)$$

This agrees with the continuum formula Eq.(12) if the small q limit is taken, $\exp(iq/2)\approx 1\approx\cos(q/2)$ and $2\sin(q/2)\approx q$. Computed behavior based on this formula will be shown in the next section, based on the Debye model.

The results developed above enable predictions of $\nabla_x T(\ell+\frac{1}{2})$ and $T(\ell)$ for any given input $\dot{e}(\ell)$. The idea is to use Eqs.(5, 7) to give

$$\begin{aligned}\nabla_x T(\ell+\frac{1}{2}) &= -\sum_{q\neq 0} e^{iq(\ell+\frac{1}{2})}J_x(q)/\kappa(q) \\ &= -\sum_{q\neq 0} e^{iq\ell}\frac{\dot{e}(q)}{(1-e^{-iq})\kappa(q)},\end{aligned} \quad (21)$$

where the second line follows from the first by using Eq.(17). This can be evaluated using Eq.(20) for $\kappa(q)$. Using Eq.(16), the temperature $T(\ell)$ can also be evaluated, from

$$T(\ell) = T_0 + \sum_{q\neq 0} e^{iq\ell}\frac{\dot{e}(q)}{4\sin^2(q/2)\kappa(q)}, \quad (22)$$

where T_0 is the average temperature. The $q=0$ term of these sums is omitted because Eqs.(2,3) make it clear that $\nabla_x T(q=0) = \sum_\ell \nabla_x T(\ell) = 0$, and similarly for $\dot{e}(q=0)$.

Two approximations have been made. One is the RTA. The other is discretization error. Temperature is a statistical variable, not definable except by averaging over a finite volume. Therefore, discretization over a finite width should not cause noticable error. However, a problem arises because gas theory has been forced to conform to the slab/junction dichotomy of the discrete picture. This causes the current in the $\ell+\frac{1}{2}$ junction to be tied to the temperature both of the two slabs $\ell+1$ and $\ell+2$ to the right, minus the temperature of both of the two slabs ℓ and $\ell-1$ to the left. This should not be a problem for gas theory, since the theory requires mean free paths longer than the small atomic dimensions used for slab widths. Only if mean free paths are shorter than interatomic spacings (that is, a liquid rather than gas limit) is the current unaware of the temperature beyond the two slabs adjacent to the junction. Nevertheless, a problem arises when the heat input $\dot{e}(\ell)$ is confined to a single site ($\ell=0$ for example.) Then discretization introduces singular responses in the form of absurd oscillations in the (unphysical) limit of very short mean free path. This problem can be cured by distributing the heat input over three slabs. Specifically, the cure is to use $\dot{e}(\ell)=\dot{e}/2$ when $\ell=0$, and $\dot{e}/4$ when $\ell=\pm 1$. This modification

has more "realism" than a single-site input. Still, it is surprising that it is required in order for gas theory to work smoothly in a slab model. Within the homogeneous slab model, the discrete non-local conductivity (Eq. 4) is an exactly defined concept, as is its Fourier representation $\kappa(q)$. Equations (21,22) are exact connections within linear response, while Eq. 20 uses the PBE, plus a further (and not essential) simplification, the RTA.

V. DEBYE MODEL

Computational theory has gone beyond the Debye model. Full solution of the PBE using accurate phonon properties from density functional theory is now widely available[23]. Nevertheless, it is useful to have a simplified model as a standard to compare real calculations against. The Brillouin zone is replaced by a sphere of radius $Q_D = (6\pi^2 n)^{1/3}$, where n is the number of atoms per unit volume. There are three branches of phonons, approximated by $\omega_Q = v|\vec{Q}|$ with the velocity v the same for each branch, and $\vec{v}_Q = v\vec{Q}/|\vec{Q}|$. The maximum frequency phonon ($\omega_{Q,\max} = \omega_D = vQ_D$) occurs at the edge of the Debye sphere where $|\vec{Q}| = Q_D$. To establish a notation, the specific heat can be written as

$$C(T) = C_\infty \int_0^{\omega_D} d\omega c(\omega) \tag{23}$$

where $c(\omega) = \mathcal{D}(\omega)E(\omega)$, and $C_\infty = 3nk_B$ is the high T classical value of $C(T)$. The factor $\mathcal{D}(\omega)$ is the phonon density of states, normalized to 1. In Debye approximation, this is $\mathcal{D}_\mathcal{D}(\omega) = 3\omega^2/\omega_D^3$. The other factor is $E(\omega) = [(\hbar\omega/2k_BT)/\sinh(\hbar\omega/2k_BT)]^2$, the Einstein formula for the specific heat (in units k_B) of one vibrational mode. This is replaced by the classical limit $E = 1$ when comparing with classical MD results.

In the spirit of the Debye model, the mean free path $\Lambda_Q = v\tau_Q$ can be modeled as $\Lambda/\Lambda_{\min}(T) = (Q_D/|\vec{Q}|)^p$, or equivalently, $(\omega_D/\omega)^p$. The exponent p depends on details of scattering. For point impurities such as isotopic substitutions, p takes the Rayleigh value $p = 4$. For anharmonic Umklapp scattering, Herring[15] has argued that usually $p = 2$, but 3 is also allowed, and both $p = 3$ and $p = 4$ have some support from numerical calculations[16,17]. The minimum mean free path, $\Lambda_{\min}$ is found at $|\vec{Q}| = Q_D$. It has a temperature-dependent value, scaling as $1/T$ from anharmonic scattering in the classical high T limit.

First consider the continuum theory. The Debye version has a simple answer in the unphysical case of $p = 0$, where all phonons have the same mean free path, $\Lambda_{\min}$. From Eq.(12), the answer is

$$\kappa_{D,p=0}(k) = \kappa_0(T)g(k\Lambda_{\min}). \tag{24}$$

Here $\kappa_0(T) = \kappa_{D,p=0}(k \to 0) \equiv \frac{1}{3}C(T)v\Lambda_{\min}(T)$ is the macroscopic result for sample size $L \to \infty$ which is the same as $k \to 0$. The function $g(k\Lambda_{\min}) = g(u)$ is defined as

$$g(u) = \frac{3}{2}\int_{-1}^{1} d\cos\theta \frac{\cos^2\theta}{1 + iu\cos\theta} = \frac{3(u - \tan^{-1}u)}{u^3}. \tag{25}$$

The variable of integration, $\cos\theta$, is the cosine of the angle between the (3-d) phonon wavevector $\vec{Q}$ and the direction $\hat{x}$ of the applied temperature gradient. The function $g(u) = \kappa_{D,p=0}(k)/\kappa_0(T)$ is plotted in Fig. 3 for the case where $\Lambda_{\min} = 10$ in units of the slab thickness A. In the small k limit, the value is $g \approx 1 - 3u^2/5$.

Eq.(24) for the more physical case of $p > 0$ becomes

$$\frac{\kappa_{D,p}(k)}{\kappa_\infty} = \frac{(3-p)}{3}\int_0^{\omega_D} d\omega c(\omega)\left(\frac{\omega_D}{\omega}\right)^p g\left(k\Lambda_{\min}\left(\frac{\omega_D}{\omega}\right)^p\right), \tag{26}$$

where $\kappa_\infty = C_\infty v\Lambda_{\text{eff}}(T)/3$ is a convenient scale factor. The "effective" mean free path, Λ_{eff} is defined as the value taken by $\kappa(k)$ in the limit $k \to 0$, namely

$$\Lambda_{\text{eff}}(T) \equiv \frac{\int d\omega c(\omega)\Lambda(\omega)}{\int d\omega c(\omega)}. \tag{27}$$

In the high temperature or classical limit where $E(\omega) = 1$ and $c(\omega) = \mathcal{D}(\omega)$, the value of Λ_{eff} is $3\Lambda_{\min}(T)/(3-p)$. For exponent $p \geq 3$, this formula no longer works. There is a well-known divergence in the ω-integral, Eq.(26) (logarithmic at $p = 3$ and worse at higher p.) The divergence is physical. If the sample is infinitely long, and the growth of mean free path with $1/\omega$ sufficiently fast ($p \geq 3$), the thermal conductivity actually diverges. In reality, this cut off by finite sample size. A simple cutoff is the minimum wavevector $k_{\min} \approx 1/L$, or a minimum frequency $\omega_{\min} \approx v/L$. But the finite sample size introduces a complication. The boundaries destroy the homogeneity of the theory. Phonons with k significantly larger than $k_{\min}$ have $\Lambda > L$, and carry heat ballistically, unaware of the spatial variation of sample temperature $T(x)$. To first approximation, this gives a lower limit ($\omega(\Lambda = L)$) below which the integral Eq.(26) is cut off. Phonons with $\omega_{\min} < \omega < \omega(\Lambda = L)$ give an extra ballistic current beyond the Fourier law. This contribution can be important at low T, but not at higher T where such phonons are a very small minority and the ballistic component is negligible.

The Debye model can also be used to find expressions for the non-local conductivity $\kappa(q)$ of the periodic slab model. First take the unphysical model with constant mean free path ($p = 0$). Using Eq.(20), the analog of Eq.(24) is

$$\kappa_{D,p=0}(q) = \kappa_0(T)h'(q, \Lambda_{\min}) = \kappa_0(T)h(w) \tag{28}$$

where $h'(q, \Lambda_{\min}) = h(w)$ is

$$h(w) = \frac{3\cos(q/2)}{2}\left[\int_0^1 d\cos\theta \frac{\cos^2\theta}{e^{iq/2} + iw\cos\theta}\right.$$

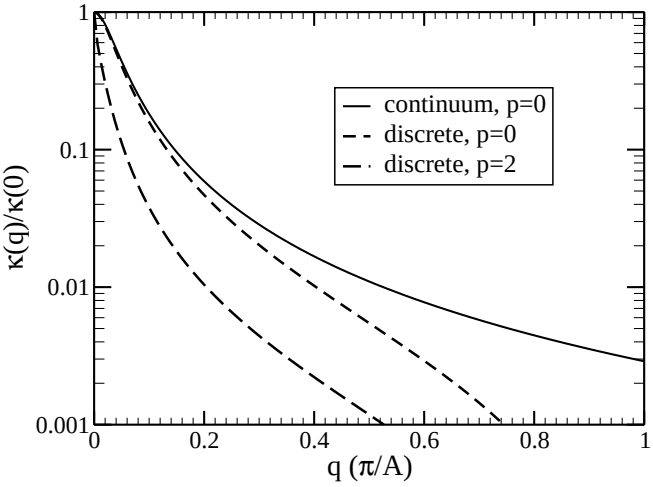

FIG. 3. Thermal conductivity *versus* wavevector, computed in Debye approximation for $\Lambda_{\rm min} = 10A$, and plotted versus wavevector $0 \le q \le \pi/A$. The top curve is the continuum model, Eqs.(24,25) with constant mean free path $\Lambda = \Lambda_{\rm min}$. The middle curve is for the discrete model, Eq.(28) with constant mean free path $p = 0$. The bottom curve, from Eq.(31), uses a more realistic frequency-dependent mean free path, with $p = 2$.

$$+ \int_{-1}^{0} d\cos\theta \frac{\cos^2\theta}{e^{-iq/2} + iw\cos\theta}\Bigg]. \qquad (29)$$

Here $w = 2\sin(q/2)\Lambda_{\rm min}$ is the discretized version of $u = k\Lambda_{\rm min}$ that appears in Eq.(25). Note that, although h depends separately on q and on $\Lambda_{\rm min}$, the additional q-dependence beyond that contained in w plays only the role of a fixed parameter, while the w dependence acquires additional importance when the mean-free path Λ_Q acquires ω_Q-dependence.

Performing the $d\cos\theta$ integral gives

$$h(w) = \frac{3\cos(q/2)}{w^3}\Re\left\{we^{iq/2} + ie^{iq}\log\left[1 + iwe^{-iq/2}\right]\right\}. \qquad (30)$$

This reduces to Eq.(25) in the small q limit, under the replacements $q \to k$ and $w \to u$. The function $h = \kappa_{D,p=0}(q)/\kappa_0(T)$ is also shown in Fig. 3. Up until $q \approx 0.2\pi$ ($q \approx 2\pi/\Lambda$) the discrete and continuum versions fall almost equally rapidly with q to < 0.1. Beyond, the discrete case falls increasingly rapidly, going to 0 at the zone boundary, $q = \pm\pi/A$. This means, for example, that there is no response to input heating $\dot{e}(\ell) = \dot{e}\exp(\pm i\pi\ell) = (-1)^\ell\dot{e}$. The reason is that adjacent junctions have currents $J(\ell+\frac{1}{2}) = \pm\dot{e}/2$. Therefore, the slab current (the average of the two adjacent junction currents) is zero.

For the more physical case of $p > 0$, the answer is

$$\frac{\kappa_{D,p}(q)}{\kappa_\infty} = \frac{(3-p)}{3}\int_0^{\omega_D} d\omega c(\omega)\left(\frac{\omega_D}{\omega}\right)^p h\left(q\Lambda_{\rm min}\left(\frac{\omega_D}{\omega}\right)^p\right) \qquad (31)$$

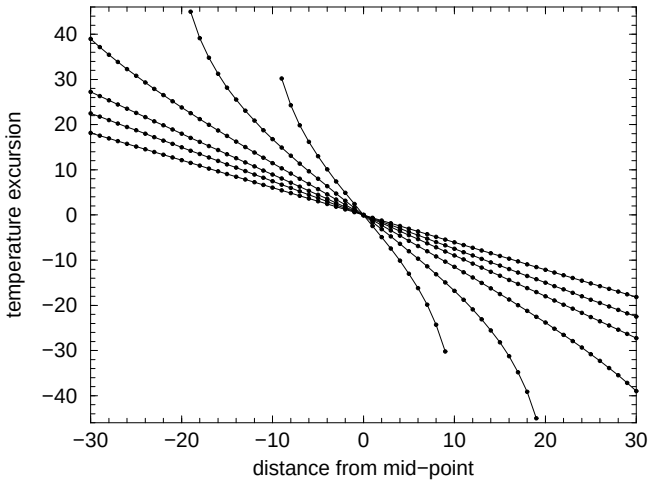

FIG. 4. Temperature *versus* distance from the midpoint $\ell = N/4$ between hot ($\ell = 0$) and cold ($\ell = N/2$) points. All computations used the discrete slab formula (Eq.(31)) and $\Lambda_{\rm min} = 20$. The power law $1/\tau_Q$ is ω_Q^2. The cell size N was 40 for the steepest curve, then 80, 160, 320, 640, and 2560.

The function $\kappa_{D,p=2}(q)/\kappa_\infty$ is shown in the classical limit ($c(\omega) = \mathcal{D}(\omega)$) in Fig. 3 as the bottom curve. The conductivity falls more much rapidly with q, which means increased non-locality. This is not surprising. Spatial memory extends much farther because of the longer mean free paths. These results are translated back to coordinate space in Fig. 2. The $p = 0$ (constant Λ) results fall exponentially (as $\exp(-m/\Lambda)$) if the supercell size NA exceeds Λ sufficiently. The $p = 2$ case behaves differently. At a distance $m = 8\Lambda_{\rm min} = 80$, the value of $\kappa(m)$ is $\approx \kappa(0)/8.4$, falling much more slowly than exponential.

VI. NUMERICAL RESULTS

Fig. 4 illustrates the computed spatial temperature variation for the discrete slab model. The behavior closely resembles that found by Zhou *et al.*[10] in their classical MD simulation of GaN. Therefore, I believe that the PBE, as extended here to discrete slabs, and modeled in RTA and in the Debye approximation, correctly captures the physics. The calculations of Fig. 4 use the classical limit $C(T) = C_\infty$, with mean free path $\Lambda = \Lambda_{\rm min}(\omega_D/\omega)^2$, $\Lambda_{\rm min} = 20A$, and various total cell lengths L ranging from $40A$ to $2560A$. Symmetry requires $T(N/4 + m) = -T(N/4 - m)$, and an inflection point in $T(\ell)$ at $\ell = N/4$. At the largest N shown, the distance $N/4$ between heat input and sink is $32\Lambda_{\rm min}$, and the answer for $\kappa_{\rm eff}(N)$ is still 10% lower than the macroscopic ($N \to \infty$) limit. The temperature profile is accurately linear, over the 60 slabs shown, for the three largest lengths L, but the slopes are 10 to 30% higher than the macroscopic limit.

Zhou *et al.*[10] invoke a Mattheissen's rule justifica-

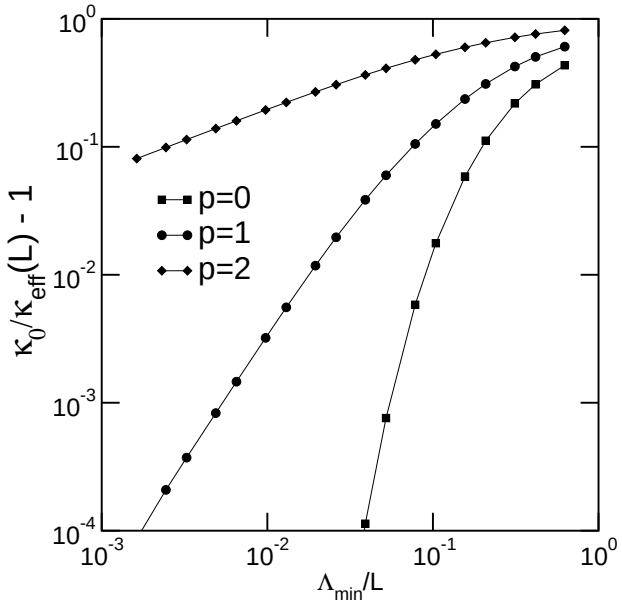

FIG. 5. Rate of convergence of $1/\kappa_{\rm eff}(L)$ to its $L \to \infty$ limit, by a logarithmic plot as a function of Λ_{min}/L. All computations used the discrete slab formula (Eq.(31)) and $\Lambda_{\rm min} = 10$. From bottom to top, the power law p of $1/\tau_Q \propto \omega_Q^p$ is $p = 0$, 1, and 2. The numerical power law of $\kappa_0/\kappa - 1 \propto (1/L)^s$ is $s \approx \infty$, 2, and 1/2.

tion for extrapolation to $L \to \infty$, namely the idea that "boundary scattering" causes $1/\kappa$ to behave like $1/\Lambda + 1/L$. However, their cell has periodic boundary conditions and therefore no actual boundary. The discrete version of the PBE presented here uses correct statistical theory and incorporates the ring geometry by design. Therefore, it should correctly describe the rate at which $\kappa_{\rm eff}(L)$ converges to the $L \to \infty$ limit, and provide guidance for extrapolation. Fig. 5 shows how $\kappa_{\rm eff}(L)$ converges as L increases. Models with constant mean free path converge exponentially, as $\exp(-4\Lambda/L)$. This is true both for continuum and discrete cases. This is not surprising, but I have not yet found a simple proof. The factor of 4 just relates to the fact that only 1/4 of the ring ($\Delta m = N/4$) is available for decay. Discrete models with mean free paths diverging as $1/\omega$ ($p = 1$) and $1/\omega^2$ ($p = 2$) are also shown in Fig. 5. They apparently converge algebraically, as $1/L^2$ for $p = 1$ and $1/\sqrt{L}$ for $p = 2$. These powers were found numerically from the slope of the log-log graphs. I conjecture that the behavior is $\kappa_{\rm bulk} - \kappa_{\rm eff}(L) \propto (1/L)^{(3-p)/p}$. This scaling for $p = 2$ is in rough accord with the highest temperature simulation by Zhou *et al.*[10], where convergence was nonlinear in $1/L$. A plot of their numerical results *versus* $1/\sqrt{L}$ instead of $1/L$ gives a significantly better linear behavior.

VII. DISCUSSION

Heat transport is generally non-local. This is seldom[1] discussed. The non-locality is hidden if the temperature gradient is uniform. Then the form of the non-locality (contained in $\kappa(k)$ for a homogeneous system) is irrelevant, since only the $k \to 0$ limit is seen. The PBE contains a valid description of non-local response, provided the carrier mean free path is sufficiently long that a quasiparticle gas description is valid. The work described in this paper uses phonon gas theory, as contained in the PBE, to describe the non-locality. The PBE is reformulated for finite size systems with periodic boundary conditions. Periodicity eliminates the distinction between ballistic and diffusive components of the current, and guarantees that a non-local Fourier law applies. Discretization into parallel slabs is natural for one-dimensional transport. The resulting $\kappa(q)$ (Eq.(31)) has, I believe, negligible discretization error, and correctly includes the nanoscale corrections that enter when mean free paths are comparable to the simulation cell length L in an MD simulation. This situation is hard to avoid for materials with good crystalline order and weak anharmonicity, such as the GaN simulation of ref. 10.

It is natural to wonder how far the periodic picture can be pushed. Discretization can obviously be done in three-dimensional fashion, giving a Fourier law with a non-local response $\kappa_{\alpha\beta}(\vec{\ell}, \vec{m})$. Can finite size complexity, such as interface temperature jumps ("Kapitsa resistance"), be correctly described by a non-local κ?

Picturing heat transport as explicitly non-local may have benefits. For example, in MD simulations of κ by the "direct method," it would be sensible to impose heat in a periodic fashion, $\dot{e}(\ell) = \cos(2\pi\ell/N)$, or $\dot{e}(q)$ containing only the smallest non-zero $q = 2\pi/N$ allowed. This simplifies Eqs.(21,22). More important, it should enable extrapolation to the $q \to 0$ limit more smoothly. Equally important, it should help reduce the noise level of MD simulations, because the "measured" $T(\ell)$ would be used at all ℓ to extract $T(q)$, rather than using only a few points of $T(\ell)$ to extract a gradient at the midpoint. A future paper on this topic is planned.

A number of recent papers formulate theories of heat conductivity in nanoscale systems[18–20]. Microscopic theory is needed, not just to supplement simulation, but more importantly, to aid experiment in interpreting nanoscale effects. Non-local effects are evident in heat transport by nanoscale samples of good conductors like graphene. Landauer methods[21–23] are often preferred, but have limitations when inelastic scattering is present. Meir-Wingreen-type[24] approaches often used to supplement Landauer methods in electron transport, and can be generalized to heat transport[19]. The PBE, which is evidently useful to model non-locality, and includes inelasticity, can perhaps be exploited in new ways to simplify and unify some of these problems.

VIII. ACKNOWLEDGEMENTS

This work was suggested by discussions with M.-V. Fernandez-Serra and J. Siebert, whose stimulation is gratefully acknowledged. I also thank D. Broido, G. Chan, Y. Li, K. K. Likharev, J. Liu, S. Ocko,T. Sun, and R. M. Wentzcovitch for helpful input. This work was supported in part by DOE grant No. DE-FG02-08ER46550.

* philip.allen@stonybrook.edu

[1] G. D. Mahan and F. Claro, Phys. Rev. B **38**, 1963 (1988).
[2] C. Dames and G. Chen, Thermal Conductivity of Nanostructured Thermoelectric Materials, CRC Handbook, edited by M. Rowe (Taylor and Francis, Boca Raton, FL, 2006), Ch. 42.
[3] G. Chen, *Nanoscale energy Transport and Conversion*, Oxford University Press, 2005, Ch. 7.
[4] Z. M. Zhang, *Nano/Microscale Heat Transfer*, McGraw-Hill, New York, 2007, Ch. 5.
[5] D. G. Cahill, W. K. Ford, K. E. Goodson, G. D. Mahan, A. Majumdar, H. J. Maris, R. Merlin, and S. R. Phillpot, J. Appl. Phys. **93**, 793 (2003).
[6] A. Majumdar, J. Heat Transfer **115**, 7 (1993).
[7] D. N. Payton, M. Rich, and W. M. Visscher, Phys. Rev. **160**, 706 (1967).
[8] F. Müller-Plathe, J. Chem. Phys. **106**, 6082 (1997).
[9] A. Maiti, G. D. Mahan, and S. T. Pantelides, Solid State Commun. **102**, 517 (1997).
[10] X. W. Zhou, S. Aubry, R. E. Jones, A. Greenstein, and P. K. Schelling, Phys. Rev. B **79**, 115201 (2009).
[11] B.-Y. Cao and Y.-W. Li, J. Chem. Phys. **133**, 024106 (2010).
[12] R. Peierls, Ann. Phys. **3**, 1055 (1929).
[13] J. M. Ziman, *Electrons and Phonons*, Oxford University Press, 1960.
[14] W. Li, J. Carrete, N. A. Katcho, and N. Mingo, Computer Phys. Commun., in press (2014).
[15] C. Herring, Phys. Rev. **95**, 954 (1954).
[16] A. Ward and D. A. Broido, Phys. Rev. B **81**, 085205 (2010).
[17] K. Esfarjani, G. Chen, and H. T. Stokes, Phys. Rev. B **84**, 085204 (2011).
[18] G. Lebon, H. Machrafi, M. Grmela, and Ch. Dubois, Proc. R. Soc A **467**, 3241 (2011).
[19] S. G. Das and A. Dhar, Eur. Phys. J. B **85**, 372 (2012).
[20] K. Sääskilahti, J. Oksanen, and J. Tulkki, Phys. Rev. E **88**, 012128 (2013).
[21] R. Landauer, Z. Phys. B - Condensed Matter **68**, 217 (1987).
[22] D. E. Angelescu, M. C. Cross, and M. L. Roukes, Superlattices Microstruct. **23**, 673 (1998).
[23] N. Mingo, Phys. Rev. B **68**, 113308 (2003).
[24] Y. Meir and N. S. Wingreen, Phys. Rev. Lett. **68**, 2512 (1992).